Available online at www.sciencedirect.com
ScienceDirect
Biochemical and Biophysical Research Communications 368 (2008) 923–929
BBRC
www.elsevier.com/locate/ybbrc

Proteasomal degradation of Atoh1 by aberrant Wnt signaling maintains the undifferentiated state of colon cancer

Mikayo Aragaki [1], Kiichiro Tsuchiya [1], Ryuichi Okamoto, Sanae Yoshioka, Tetsuya Nakamura, Naoya Sakamoto, Takanori Kanai, Mamoru Watanabe *

Department of Gastroenterology and Hepatology, Graduate School, Tokyo Medical and Dental University, 1-5-45 Yushima, Bunkyo-ku, Tokyo 113-8519, Japan

Received 2 February 2008
Available online 12 February 2008

Abstract

Atoh1 plays a crucial role in intestinal cell differentiation. We have demonstrated that its human homolog Hath1 protein is targeted by the Wnt-GSK3 axis, resulting in the proteasomal degradation in human colon cancer. However, the contribution of Hath1 degradation to the undifferentiated state of colon cancer remains unknown. In this study, we demonstrated that both constitutive expression of mutant Hath1 and stabilization of Hath1 protein by a GSK3 inhibitor in colon cancer cells increased the expression of MUC2 known as a representative function of differentiated goblet cells. This means that Hath1 protein degradation may be required for maintaining the undifferentiated state of colon cancers, and that GSK3 inhibitors have potential for use in cancer therapy.

Keywords: Atoh1; Hath1; Proteasomal degradation; Differentiation; Wnt; GSK3β; Colon cancer

Atoh1 is a bHLH transcriptional factor that plays a critical role in terminal cell differentiation of intestinal epithelium, dorsal interneuron in the spinal cord, granule cells in the cerebellum, and inner hair cells in the auditory systems [1–4]. The mouse homolog of Atoh1, Math1, is expressed in the central nervous system and intestine in embryos but confined to the intestine in adults [5]. In Math1-deficient mice, loss of Math1 induces depletion of secretory cells such as Paneth cells, enteroendocrine cells and goblet cells, indicating that continuous expression of Atoh1 is required for proper differentiation and maintenance of epithelial homeostasis in intestine throughout the life span [4]. The human homolog of Atoh1, Hath1, is also strongly expressed in normal colon and small intestine [6,7], suggesting that it likewise contributes to the terminal differentiation of intestinal epithelial cells.

Dysregulation of Hath1 expression is thought to induce various diseases of the intestinal tracts. Loss of Hath1 protein has been observed in colorectal cancer, where Wnt signaling is constitutively activated by the truncated mutation of the adenomatous polyposis coli gene (APC); and Hath1 mRNA expression was found to be down-regulated in some colon cancer tissues compared with normal colon [6,7]. Thus, repression of Hath1 mRNA in colon cancer might promote maintenance of the undifferentiated state. However, not all colorectal cancers show low expression of Hath1 mRNA [6–8]. We have reported that Hath1 protein was lost in colorectal cancer even in the presence of Hath1 mRNA [7].

To clarify this anomaly in the expression of Hath1 protein and mRNA in colon cancer, we have examined the regulation of Hath1 protein stability in colon cancer-derived cell lines. Our previous study demonstrated that Hath1 protein was actively degraded by the ubiquitin–proteasome system via Wnt signaling that switched the target of

Abbreviations: APC, Adenomatous polyposis coli; GSK3β, glycogen synthase kinase 3β.

* Corresponding author. Fax: +81 3 5803 0262.
E-mail address: mamoru.gast@tmd.ac.jp (M. Watanabe).

[1] Both authors equally contributed to this work.

0006-291X/$ - see front matter © 2008 Elsevier Inc. All rights reserved.
doi:10.1016/j.bbrc.2008.02.011

GSK3β from β-catenin to Hath1 in colon cancer cells [7]. Aberrant Wnt signaling by truncated APC has been highlighted as the most critical trigger for carcinogenesis in colon, being observed in approximately 80% of patients with colorectal cancer [9,10]. Although it has been supposed that the accumulated β-catenin protein resulting from the aberrant Wnt signaling induced carcinogenesis and maintained the undifferentiated state of colon cancer, we have found that the Wnt signaling induced not only the continuous expression of β-catenin protein but also proteasomal degradation of Hath1 protein. Moreover, the inactivation of Wnt signaling by forced expression of the full-length APC gene in colon cancer cells gave rise to both β-catenin protein degradation and Hath1 protein stabilization, resulting in the cell differentiation toward goblet cells [7].

These results raise questions of whether is more effective in maintaining the undifferentiated state of colon cancer, uncontrolled expression of β-catenin or proteasomal degradation of Hath1, and whether the expression of Hath1 protein alone has the potential to promote the differentiation of intestinal epithelial cells even with β-catenin accumulation promoting the proliferating state.

In this study, we aimed to elucidate the effect of Hath1 protein stability on the undifferentiated state in human colon cancer. We found that the mutant Hath1 protein in which serine residues were replaced with alanine was stably expressed in human colon cancer cells with the aberrant Wnt signaling, resulting in the induction of differentiation toward goblet cells. We also demonstrated that treatment with a GSK3 inhibitor stabilized Hath1 protein and directed the colon cancer cells toward goblet cells, suggesting that GSK3 inhibitors have potential for use in a new therapeutic approach for the majority of patients suffering from colorectal cancers.

Materials and methods

DNA constructs. Expression plasmids used for this study were generated as reported previously [7].

Cell culture and creation of transient and stable cell lines. Human colon adenocarcinoma-derived SW480, DLD-1 cells, and human embryonic kidney-derived 293T cells were cultured in Dulbecco's modified Eagle's medium (Life Technologies, Grand Island, NY) supplemented with 10% fetal bovine serum and 1% penicillin–streptomycin. In all experiments 1×10^6 cells were grown in 6-cm dishes and were transiently transfected by using TransIT transfection reagent (Mirus, Madison, WI) according to the manufacturer's protocol with 4 μg of expression plasmids. Transfected cells were cultured under the usual conditions or in the presence of 10 μmol/L MG132 (Calbiochem) or 100 mmol/L LiCl (Sigma–Aldrich). Stable cell lines in DLD-1 were constructed with the Tet-On system with tet-repressor, pcDNA4-Flag Hath1 or Flag SA Hath1 plasmids. For selection, both blasticidin (7.5 μg/ml) and zeocin (750 μg/ml) were added for WT and SA cells. Hath1 gene expression was induced by cultivation in the presence of doxycycline for 12 h or more. After cultivation with doxycycline, MG132 (10 μmol/L) was added to the media and cultivation was continued for 8 h.

Western blot analysis. Cells were extracted with 1% sodium dodecyl sulfate (SDS)-containing radioimmunoprecipitation assay (RIPA) buffer as previously described [7]. The supernatants were removed and quantitated using protein assay reagent (Pierce, Rockford, IL). Preparations of 50 μg or 100 μg of proteins were separated in 12% SDS–polyacrylamide gels, transferred to polyvinylidene difluoride (PVDF) membranes according to standard procedures. The membranes were immunoblotted with anti-Flag M2 (Sigma Chemical Co., St. Louis, MO), anti-β-catenin (BD Biosciences Pharmingen), and anti-USF2 (Santa Cruz Biotechnology), then incubated with the secondary antibodies.

Luciferase assays. 293T cells were transiently transfected with 10 ng of *Renilla* luciferase reporter plasmid pRL-TK-Luc (Promega) along with 100 ng of either E-box-Luc or MUC2-Luc reporter plasmid and 100 ng of the expression plasmids. The data are represented as total relative light units (RLU) on histograms showing the average ± SEM of triplicate determinations.

Real-time PCR. SW480 cells were transiently transfected as indicated previously, then stimulated with 100 mmol/L LiCl for 8 h. DLD-1cells with the Tet-On system were stimulated with doxycycline for 5 d. Total RNA was isolated using TRIzol reagent (Invitrogen). Aliquots of 1 μg of total RNA were used for reverse transcription (Qiagen). Quantitative polymerase chain reaction was carried out using lightcycler (Roche) in triplicate to measure mRNA expression of Mucin2 (MUC2), Hath1, c-myc, and CDX2. The following Hath1 and CDX2 specific primers were used: Hath1 forward primer 5′-GCC CAA ATC TAC ATC AAC GCC-3′; Hath1 reverse primer 5′-TTG CCC GCG CCC CCT TCA TAG-3′; CDX2 forward primer 5′-CGG CTG GAG CTG GAG AAG G-3′; and CDX2 reverse primer 5′-TCA GCC TGG AAT TGC TCT GC-3′. Primers for MUC2 and c-myc were as described previously [7].

Immunocytochemistry. DLD-1 Tet-On cells were incubated in MG132 for 8 h following stimulation by doxycycline for 12 h, were fixed with 2.0% paraformaldehyde and were permeabilized with 0.5% Triton-X in PBS. Anti-Flag M2 antibody diluted with PBS was utilized to detect Flag-tagged Hath1. Incubation with anti-mouse IgG HRP-linked whole antibody (Amersham Biosciences) as the secondary antibody followed.

Results

A mutant Hath1 protein showed enhanced protein stability while maintaining its transcriptional activity in colon cancer cells

To determine the contribution of Hath1 protein stability to cell differentiation of colon cancer, we first attempted to express Hath1 protein stably in colon cancer cells. We have previously confirmed the protein stability of various mutant Hath1 constructs in colon cancer cells and found the critical region for Hath1 degradation to be the 54th and 58th serine residues of Hath1 protein [7]. The mutants represented in Fig. 1A were as follows. N1 and N5 are N-terminal deletion mutants of Hath1 preserving or excluding the critical serine residues, respectively. SA is a mutant in which the 54th and 58th serine residues are replaced with alanine residues (Fig. 1A). Wild-type (WT) and mutants of Hath1 transiently transfected into 293T cells with inactive Wnt signaling were confirmed to express all proteins stably (Fig. 1B). When transfected into the human colon cancer cell line with active Wnt signaling, both WT and N1 were degraded by the ubiquitin–proteasome system, while both N5 and SA were stably expressed even in the absence of the proteasome inhibitor MG132, as previously found (Fig. 1C). Although it has been reported that Hath1 binds to E-box sequences to activate the transcription of target genes [5], the critical region for the transcriptional activity of Hath1 remains unknown. We therefore per-

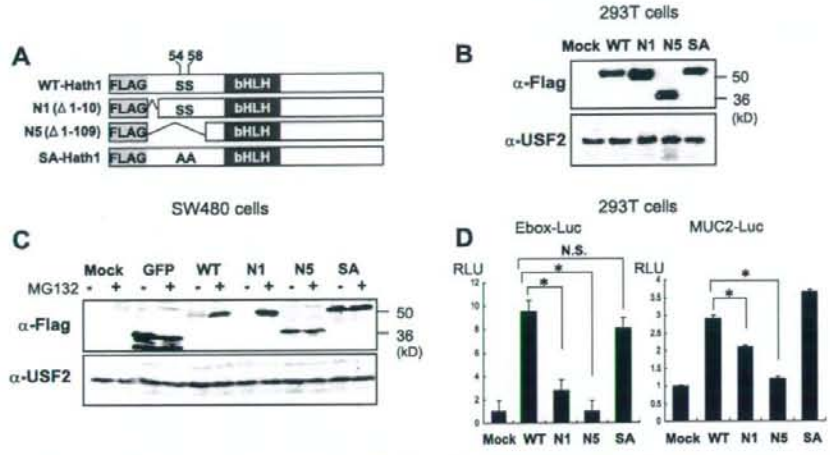

Fig. 1. Hath1 protein induced by alanine-substituted mutant showed enhanced stability while maintaining its transcriptional activity. (A) Schematic representation of various Flag-tagged Hath1 mutants used in this study. The N-terminal deleted regions of each mutant are designated by amino acid numbers. Serine residues at positions 54 (S54) and 58 (S58) are indicated. (B) 293T cells in which Wnt signaling is inactive were transfected with two of the N-terminal deletion mutants and a substituted mutant of Hath1 in addition to the WT. (C) SW480 cells were transfected by the same procedure as (B). WT and N1 mutant preserving the critical regions for protein degradation were detected only in the presence of MG132. N5 and SA lacking the critical regions expressed the proteins without the reagent. (D) 293T cells were co-transfected with of each of the WT and Hath1 mutants and either E-box Luc or MUC2 Luc. $^{*}P < 0.05$.

formed the luciferase assay with the Hath1 mutants in 293T cells (Fig. 1D). SA showed equivalent transcriptional activity to the wild-type, while N1 and N5 showed significantly reduced transcriptional activity, implying that the critical region for the transcriptional activity lies at the N-terminus of Hath1. Moreover, previous studies have noted a close association of Hath1 with MUC2 gene expression [6–8] and the transactivation of MUC2 promoter by Hath1 [8]. We found that SA and WT Hath1 showed equivalent transcriptional activity of MUC2, while N1 and N5 lost this activity (Fig. 1D).

Stable expression of SA Hath1 increases its transcriptional activity

Since only the SA mutant of Hath1 was stably expressed while maintaining its transcriptional activity in colon cancer cells, we considered that SA Hath1 was suitable to assess whether Hath1 has the potential to promote differentiation in colon cancer. We then constructed a cell line stably expressing the SA Hath1 protein through the Tet-On system in which expression of a target gene is induced by doxycycline. Expression of WT Hath1 protein was not induced by doxycycline alone, while SA was expressed regardless of treatment with MG132 (Fig. 2A). Moreover, immunofluorescence analysis revealed that SA Hath1 protein was expressed in the nucleus even in the absence of MG132 (Fig. 2B). Next, we examined the E-box-dependent transcriptional activity of SA Hath1 in colon cancer cells. Luciferase assay showed that the transcriptional activity of SA Hath1 is notably higher than of WT Hath1, possibly because of the increased amount of protein bound to E-box sequences (Fig. 2C).

Stable expression of SA Hath1 induces MUC2 mRNA on active Wnt signaling

Because the transcriptional activity of SA Hath1 was higher than of WT Hath1 in colon cancer cells, we further investigated whether constitutive Hath1 protein expression could induce differentiation characteristics in colon cancer cells. MUC2 mRNA expression was significantly up-regulated by the stable expression of SA Hath1 with doxycycline stimulation for 5 d, suggesting that SA Hath1 protein might induce the differentiated state of colon cancer cells (Fig. 3A). On the other hand, WT Hath1 was actively degraded by the proteasome system, resulting in the invariable expression of MUC2 mRNA. Next we examined whether MUC2 expression in colon cancer cells was related to the up-regulation of CDX2, since transcription of the MUC2 gene is reported to be induced by CDX2 binding to the MUC2 promoter [11]. Quantitative real-time RT-PCR assay revealed that CDX2 mRNA was not up-regulated, suggesting that MUC2 mRNA up-regulation by stable expression of Hath1 was independent of CDX2 in colon cancer cells (Fig. 3B). Importantly, Wnt signaling in SA Hath1 stable cell line is as active as in naive cells, because the amount of β-catenin and the expression of c-myc, which is one of the target genes of Wnt signaling, did not change in any of the cells (Fig. 3C and D). Together, these results indicate that stable Hath1 protein is itself sufficient to induce MUC2 mRNA without the

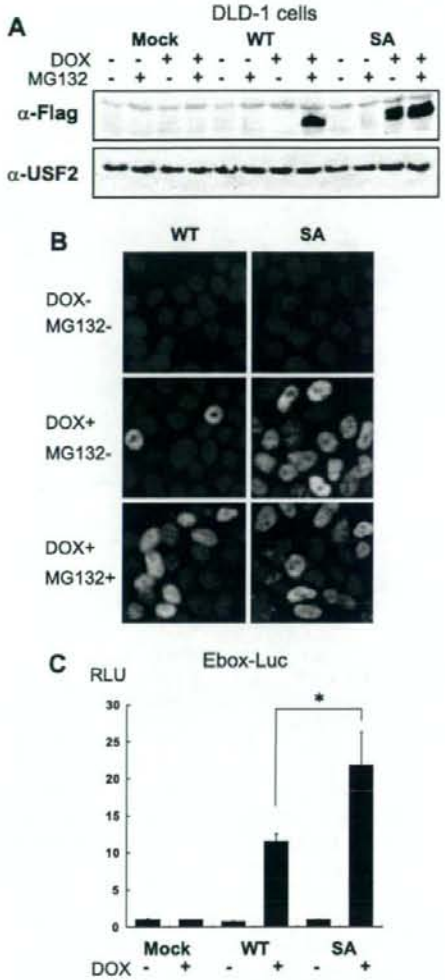

Fig. 2. DLD-1 stable cell line inducible for mutant SA Hath1 expression has increased transcriptional activity. (A) DLD-1 Tet-On cells were stimulated with doxycycline for 12 h before the incubation with MG132. (B) Immunocytochemical analysis of DLD-1 Tet-On cells in which expression from transfected SA Hath1 was performed to detect the SA Hath1 protein in the nucleus with or without MG132. (C) Luciferase assay was performed in DLD-1 Tet-On cells transfected with E-box Luc reporter plasmid. $^{*}P < 0.05$.

influence on constitutive expression of a group of target genes of β-catenin/TCF4 driving cell proliferation.

The GSK3 inhibitor stabilizes Hath1 protein, leading to up-regulation of MUC2 mRNA in colon cancer cells

As results suggested that SA Hath1 protein stably expressed in colon cancer cells was responsible for MUC2 mRNA expression, we investigated whether WT Hath1 stabilized by GSK3 inhibitors is able to induce MUC2 mRNA expression without the repression of Wnt signaling. Hath1 protein was detected in colon cancer cells incubated with a GSK3 inhibitor, LiCl, while the amount of β-catenin protein accumulated in the cells remained unchanged (Fig. 4A). Interestingly, WT Hath1 stabilized by LiCl increases MUC2 mRNA expression, suggesting that the stabilization of Hath1 protein is essential to induce definitive intestinal differentiation without the suppression of Wnt signaling in colon cancer cells (Fig. 4B).

Discussion

The results of this study demonstrate the significance of Hath1 protein stabilization in regulating the differentiation state of human colon cancer. We found that a Hath1 mutant in which serine residues were replaced with alanine (SA Hath1) is capable of stable expression while maintaining its transcriptional activity in colon cancer cells, and the N-terminus of Hath1 is essential for the E-box-dependent transcriptional activity. We demonstrated that the stable expression of SA Hath1 up-regulates its transcriptional activity, possibly through an increase in the amount of protein bound to E-box sequences. This results in increased expression of MUC2 mRNA, even in cells with accumulated β-catenin protein, which gives rise to the proliferated state. We further showed that the stabilization of WT Hath1 protein by a GSK3 inhibitor is adequate for the up-regulation of MUC2 mRNA in colon cancer cells, and propose that degradation of the Hath1 protein might lead to the undifferentiated state in colon cancer.

The significant role of Wnt signaling in healthy and malignant intestinal epithelium has been noted in terms of maintenance for both continuous proliferated and undifferentiated states [12,13]. Active Wnt signaling simultaneously promotes cell proliferation and inhibits differentiation through controlling c-myc and $p21^{CIP/WAF1}$ activity [13]. Our concern has been to find whether suppression of cell proliferation by inactivation of Wnt signaling leads exclusively the differentiated state in colon cancer. Focusing on the role of Hath1 in intestinal cell differentiation and its regulation at protein level, we contribute a new aspect to the establishment of neoplastic characteristics. Our findings in this study first suggest a partial contribution of Hath1 protein to the undifferentiated state in colon cancer. Hath1 protein degradation by active Wnt signaling might cause cell differentiation to halt, giving rise to the undifferentiated state viewed as one of characteristics of colon cancer. Our results are supported by the fact that, although Hath1 protein is expressed in only 7% of nonmucinous carcinomas, both Hath1 and MUC2 are expressed in more than 70% of mucinous cancers which have low malignant potential without APC deletion [8]. However, stabilization of Hath1 protein did not induce other differentiation markers such as phospholipase A2 (sPLA2), isomaltase and chromogranin A (CgA), in spite of the possibility of differentiation toward three secretory lineages

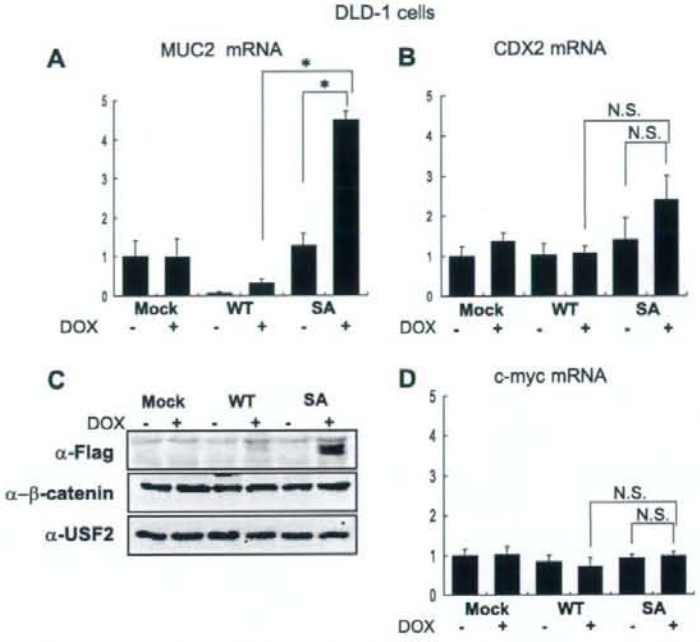

Fig. 3. Stabilization of Hath1 protein generates MUC2 mRNA independently of active Wnt signaling. (A) DLD-1 Tet-On cells were stimulated with doxycycline for 5 d. Results are expressed as the ratio of the levels of MUC2 mRNA to β-actin mRNA. $^{*}P < 0.05$. (B) (D) The same samples as in (A) were used to investigate CDX2 and c-myc mRNA expression, respectively. Results are expressed as the ratio of the levels of CDX2 and c-myc mRNA to β-actin mRNA. $^{*}P < 0.05$. (C) DLD-1 Tet-On cells were stimulated with doxycycline for 12 h. Immunoblotting was done with anti-β-catenin antibody.

(data not shown). The extent of the Hath1 contribution should be further analyzed.

Another important point of view in this study concerns the first phase of carcinogenesis. APC mutation has been revealed to promote the first stage initiation of carcinogenesis [14]. Immunohistochemical analysis of Hath1 protein expression in normal colon tissue by [6,7] suggests that APC mutation in colon cells might promote not only stable expression of β-catenin but also proteasomal degradation of Hath1 protein, leading to diminishment of Hath1 mRNA and resulting in the establishment of the undifferentiated state of cancer in the end stage. Therefore, in the early stage of carcinogenesis by APC deletion, the degradation of Hath1 protein is thought to be more essential than the diminishment of Hath1 mRNA in producing the undifferentiated state.

We finally propose that GSK3 inhibitors have potential for use in a new approach for anti-colon cancer drugs. Although many alternative therapies have been targeted to the Wnt signaling axis [15–17], development of a drug that targets Wnt signaling is difficult because of the complexity of the protein–protein interactions [15].

GSK3 is considered as a key enzyme in various neoplasms. Since many transcriptional factors, cell cycle regulators and proto-oncogenes act as substrates for GSK3, GSK3 has been considered as a suppressor of cellular neoplastic transformation [18]. Therefore, it has been suggested that GSK3 inhibitors might increase the risk of carcinogenesis [18,19]. LiCl, a relatively specific inhibitor of GSK3, has been used in therapies for bipolar disorder for many years, but the risk of cancer development in psychiatric patients treated with LiCl is even lower than in the general population, suggesting that LiCl may have a protective effect against cancer [20]. Another study indicates that the GSK3 inhibitors might not be sufficient to elevate the level of β-catenin protein in normal primary cells [21].

The benefits of GSK3 inhibitor use for colorectal cancer reduction have been described [22–24]. LiCl treatment in APC^{min} mouse does not increase the number of tumors compared with control, suggesting a low risk of cancer development [22]. Treatment with GSK3 inhibitors of mouse with subcutaneous xenografts of SW480 significantly inhibits proliferation of cancer cell xenografts, with no apparent pathological changes in other major organs [23]. Although, problematically, the molecular pathways and mechanisms involved in the anti-cancer effect of GSK3 inhibitors remain unclear [22–24], we have elucidated the molecular mechanisms of a GSK3 inhibitor in the reduction of colon cancer.

In conclusion, Hath1 protein has a potential to promote the differentiation of colon cancer cells independently of β-catenin accumulation, and stabilization of Hath1 protein

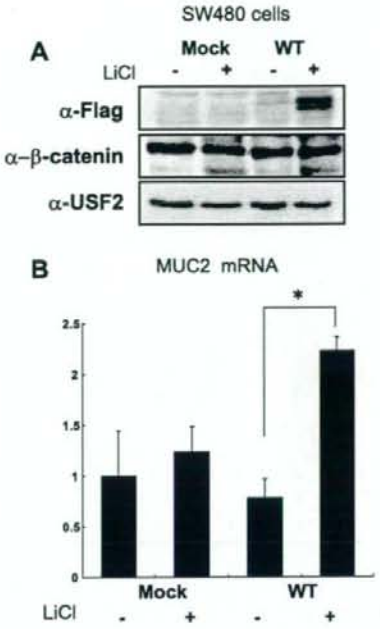

Fig. 4. The GSK3 inhibitor stabilizes Hath1 protein, leading to up-regulation of MUC2 mRNA in colon cancer cell lines. (A) SW480 cells were transiently transfected with WT Hath1 before 8 h of incubation in LiCl. Protein lysates were utilized for immunoblotting. (B) SW480 cells were transfected by the same procedure. Results of a quantitative real-time RT-PCR are expressed as the ratio of the levels of MUC2 mRNA to β-actin mRNA. $^{*}P < 0.05$.

by GSK3 inhibitors has intriguing therapeutic potential for colon cancer. Further detailed analyses of the switching mechanism of the GSK3β target between β-catenin and Hath1 on proteasomal degradation are required in order to introduce simple and pinpointed target therapies for colorectal cancers.

Acknowledgments

This work was supported in part by Grants-in-Aid for Scientific Research, and Creative Scientific Research on Priority Areas, Exploratory Research, and Creative Scientific Research from the Japanese Ministry of Education, Culture, Sports, Science, and Technology and the Japanese Ministry of Health, Labor, and Welfare.

References

[1] N. Ben-Arie, H.J. Bellen, D.L. Armstrong, A.E. McCall, P.R. Gordadze, Q. Guo, M.M. Matzuk, H.Y. Zoghbi, Math1 is essential for genesis of cerebellar granule neurons, Nature 390 (1997) 169–172.

[2] N.A. Bermingham, B.A. Hassan, S.D. Price, M.A. Vollrath, N. Ben-Arie, R.A. Eatock, H.J. Bellen, A. Lysakowski, H.Y. Zoghbi, Math1: an essential gene for the generation of inner ear hair cells, Science 284 (1999) 1837–1841.

[3] K. Gowan, A.W. Helms, T.L. Hunsaker, T. Collisson, P.J. Ebert, R. Odom, J.E. Johnson, Crossinhibitory activities of Ngn1 and Math1 allow specification of distinct dorsal interneurons, Neuron 31 (2001) 219–232.

[4] Q. Yang, N.A. Bermingham, M.J. Finegold, H.Y. Zoghbi, Requirement of Math1 for secretory cell lineage commitment in the mouse intestine, Science 294 (2001) 2155–2158.

[5] C. Akazawa, M. Ishibashi, C. Shimizu, S. Nakanishi, R. Kageyama, A mammalian helix–loop–helix factor structurally related to the product of *Drosophila* proneural gene atonal is a positive transcriptional regulator expressed in the developing nervous system, J. Biol. Chem. 270 (1995) 8730–8738.

[6] C.C. Leow, M.S. Romero, S. Ross, P. Polakis, W.Q. Gao, Hath1 down-regulated in colon adenocarcinomas, inhibits proliferation and tumorigenesis of colon cancer cells, Cancer Res. 64 (2004) 6050–6057.

[7] K. Tsuchiya, T. Nakamura, R. Okamoto, T. Kanai, M. Watanabe, Reciprocal targeting of Hath1 and beta-catenin by Wnt glycogen synthase kinase 3beta in human colon cancer, Gastroenterology 132 (2007) 208–220.

[8] E.T. Park, H.K. Oh, J.R. Gum Jr., S.C. Crawley, S. Kakar, J. Engel, C.C. Leow, W.Q. Gao, Y.S. Kim, HATH1 expression in mucinous cancers of the colorectum and related lesions, Clin. Cancer Res. 12 (2006) 5403–5410.

[9] P. Polakis, Wnt signaling and cancer, Genes Dev. 14 (2000) 1837–1851.

[10] P. Polakis, The oncogenic activation of beta-catenin, Curr. Opin. Genet. Dev. 9 (1999) 15–21.

[11] H. Yamamoto, Y.Q. Bai, Y. Yuasa, Homeodomain protein CDX2 regulates goblet-specific MUC2 gene expression, Biochem. Biophys. Res. Commun. 300 (2003) 813–818.

[12] D. Pinto, A. Gregorieff, H. Begthel, H. Clevers, Canonical Wnt signals are essential for homeostasis of the intestinal epithelium, Genes Dev. 17 (2003) 1709–1713.

[13] M. van de Wetering, E. Sancho, C. Verweij, W. de Lau, I. Oving, A. Hurlstone, K. van der Horn, E. Batlle, D. Coudreuse, A.P. Haramis, M. Tjon-Pon-Fong, P. Moerer, M. van den Born, G. Soete, S. Pals, M. Eilers, R. Medema, H. Clevers, The beta-catenin/TCF-4 complex imposes a crypt progenitor phenotype on colorectal cancer cells, Cell 111 (2002) 241–250.

[14] A.G. Renehan, S.T. O'Dwyer, N.J. Haboubi, C.S. Potten, Early cellular events in colorectal carcinogenesis, Colorectal Dis. 4 (2002) 76–89.

[15] J.H. van Es, M.E. van Gijn, O. Riccio, M. van den Born, M. Vooijs, H. Begthel, M. Cozijnsen, S. Robine, D.J. Winton, F. Radtke, H. Clevers, Notch/gamma-secretase inhibition turns proliferative cells in intestinal crypts and adenomas into goblet cells, Nature 435 (2005) 959–963.

[16] J.H. van Es, H. Clevers, Notch and Wnt inhibitors as potential new drugs for intestinal neoplastic disease, Trends Mol. Med. 11 (2005) 496–502.

[17] D.H. Palmer, M.J. Chen, D.J. Kerr, Gene therapy for colorectal cancer, Br. Med. Bull. 64 (2002) 201–225.

[18] P. Cohen, M. Goedert, GSK3 inhibitors: development and therapeutic potential, Nat. Rev. Drug Discov. 3 (2004) 479–487.

[19] A. Tighe, A. Ray-Sinha, O.D. Staples, S.S. Taylor, GSK-3 inhibitors induce chromosome instability, BMC Cell Biol. 8 (2007) 34.

[20] Y. Cohen, A. Chetrit, Y. Cohen, P. Sirota, B. Modan, Cancer morbidity in psychiatric patients: influence of lithium carbonate treatment, Med. Oncol. 15 (1998) 32–36.

[21] D.B. Ring, K.W. Johnson, E.J. Henriksen, J.M. Nuss, D. Goff, T.R. Kinnick, S.T. Ma, J.W. Reeder, I. Samuels, T. Slabiak, A.S. Wagman, M.E. Hammond, S.D. Harrison, Selective glycogen synthase kinase 3 inhibitors potentiate insulin activation of glucose transport and utilization in vitro and in vivo, Diabetes 52 (2003) 588–595.

[22] T.D. Gould, N.A. Gray, H.K. Manji, Effects of a glycogen synthase kinase-3 inhibitor, lithium, in adenomatous polyposis coli mutant mice, in adenomatous polyposis coli mutant mice, Pharmacol. Res. 48 (2003) 49–53.
[23] A. Shakoori, W. Mai, K. Miyashita, K. Yasumoto, Y. Takahashi, A. Ooi, K. Kawakami, T. Minamoto, Inhibition of GSK-3 beta activity attenuates proliferation of human colon cancer cells in rodents, Cancer Sci. 98 (2007) 1388–1393.
[24] J. Tan, L. Zhuang, H.S. Leong, N.G. Iyer, E.T. Liu, Q. Yu, Pharmacologic modulation of glycogen synthase kinase-3beta promotes p53-dependent apoptosis through a direct Bax-mediated mitochondrial pathway in colorectal cancer cells, Cancer Res. 65 (2005) 9012–9020.

Potential Relevance of Cytoplasmic Viral Sensors and Related Regulators Involving Innate Immunity in Antiviral Response

YASUHIRO ASAHINA,* NAMIKI IZUMI,* ITSUKO HIRAYAMA,* TOMOHIRO TANAKA,* MITSUAKI SATO,*,‡ YUTAKA YASUI,* NOBUTOSHI KOMATSU,*,‡ NAOKI UMEDA,* TAKANORI HOSOKAWA,* KEN UEDA,* KAORU TSUCHIYA,* HIROYUKI NAKANISHI,* JUN ITAKURA,* MASAYUKI KUROSAKI,* NOBUYUKI ENOMOTO,‡ MEGUMI TASAKA,§ NAOYA SAKAMOTO,§ and SHOZO MIYAKE*

*Department of Gastroenterology and Hepatology, Musashino Red Cross Hospital, Tokyo; ‡First Department of Internal Medicine, Faculty of Medicine, University of Yamanashi, Yamanashi; and §Department of Gastroenterology and Hepatology, Tokyo Medical and Dental University, Tokyo, Japan

Background & Aims: **Clinical significance of molecules involving innate immunity in treatment response remains unclear. The aim is to elucidate the mechanisms underlying resistance to antiviral therapy and predictive usefulness of gene quantification in chronic hepatitis C (CH-C).** ***Methods:*** **We conducted a human study in 74 CH-C patients treated with pegylated interferon α-2b and ribavirin and 5 nonviral control patients. Expression of viral sensors, adaptor molecule, related ubiquitin E3-ligase, and modulators were quantified.** ***Results:*** **Hepatic RIG-I, MDA5, LGP2, ISG15, and USP18 in CH-C patients were up-regulated at 2- to 8-fold compared with non-hepatitis C virus patients with a relatively constitutive Cardif. Hepatic RIG-I, MDA5, and LGP2 were significantly up-regulated in nonvirologic responders (NVR) compared with transient (TR) or sustained virologic responders (SVR). Cardif and RNF125 were negatively correlated with RIG-I and significantly suppressed in NVR. Differences among clinical responses in RIG-I/Cardif and RIG-I/RNF125 ratios were conspicuous (NVR/TR/SVR = 1.3:0.6:0.4 and 2.3:1.3:0.8, respectively). Like viral sensors, ISG15 and USP18 were significantly up-regulated in NVR (4-fold and 2.3-fold, respectively). Multivariate and receiver operator characteristic analyses revealed higher RIG-I/Cardif ratio, ISG15, and USP18 predicted NVR. Lower Cardif in NVR was confirmed by its protein level in Western blot. Also, transcriptional responses in peripheral blood mononuclear cells to the therapy were rapid and strong except for Cardif in not only a positive (RIG-I, ISG15, and USP18) but also in a negative regulatory manner (RNF125).** ***Conclusions:*** **NVR may have adopted a different equilibrium in their innate immune response. High RIG-I/Cardif and RIG-I/RNF125 ratios and ISG15 and USP18 are useful in identifying NVR.**

Infection with hepatitis C virus (HCV) is a common cause of chronic hepatitis, which progresses to cirrhosis and hepatocellular carcinoma in many patients.[1] Although combination therapy with pegylated interferon (PEG-IFN) α and ribavirin is now established as the standard treatment for chronic HCV infection genotype 1b, the sustained virologic response rate in these patients is still around 50%.[2–4] Moreover, physicians have also found that 20% of patients are nonvirologic responders (NVR; those whose HCV-RNA does not become negative during 48 weeks of combination therapy).[5] Prediction of NVR status is of clinical importance because these patients have no chance of achieving a sustained virologic response even after prolonged combination therapy.[6] However, mechanisms involving resistance to PEG-IFN-α and ribavirin have not been fully elucidated, and it is difficult to predict treatment responses before initiation of PEG-IFN-α and ribavirin combination therapy.

In vitro studies have suggested that an innate immune response in viral infection is an essential part of the host antiviral defense system.[7] HCV evades the host immune response through a complex combination of processes that include signaling interference, effector modulation, and continual viral genetic variation.[8] We hypothesized that liver tissue would show a consistent difference between responders and nonresponders in expression levels of the gene involved in innate immunity and IFN signal transduction. These differences could be used to predict treatment outcomes.

The retinoic acid–inducible gene I (RIG-I), a cytoplasmic RNA helicase, and the related melanoma differentia-

Abbreviations used in this paper: CARD, Caspase-recruiting domain; Cardif, caspase-recruiting domain adaptor inducing IFN-β; G3PDH, glyceraldehyde-3-phosphate dehydrogenase; HCV, hepatitis C virus; IPS-1, IFN-β promoter stimulator I; ISG15, IFN-stimulated gene 15; PEG-IFN, pegylated interferon; MDA5, melanoma differentiation associated gene 5; MAVS, mitochondrial antiviral signaling protein; NVR, nonvirologic responders; PBMC, peripheral blood mononuclear cell; RIG-I, retinoic acid-inducible gene I; RNF125, ring-finger protein 125; ROC, receiver operator characteristic; SVR, sustained viral responder; TR, transient responder; UBP43, ubiquitin-specific protease 43; USP18, ubiquitin-specific protease 18; VISA, virus-induced signaling adaptor.

0016-5085/08/$34.00
doi:10.1053/j.gastro.2008.02.019

Table 1. Patient Characteristics at Baseline According to Final Virologic Response

	SVR n = 30	TR n = 24	NVR n = 20	*P* value
Age (*y*)	52 ± 13	60 ± 8.7	60 ± 10	.04[a]
Female % (M/F)	47% (16/14)	63% (9/15)	60% (8/12)	.5[b]
Naïve & Relapser[c]/Non-responder[c]	26/4	20/4	14/6	.3[b]
BMI	24.6 ± 3.0	24.9 ± 4.4	24.0 ± 2.1	.6[a]
ALT (*IU/L*)	75 ± 57	65 ± 35	68 ± 41	1.0[a]
Hemoglobin (*g/dL*)	14.3 ± 1.6	14.1 ± 1.1	14.5 ± 1.7	.6[a]
Platelet count ($\times 10^3/\mu L$)	182 ± 62	169 ± 48	140 ± 39	.04[a]
Liver histology				
A1/A2/A3	19/8/3	14/8/1	10/10/0	.3[b]
F1/F2/F3	14/9/7	11/7/5	7/5/8	.7[b]
Viral load ($\times 10^6$ *IU/mL*)	1.6 ± 1.2	1.8 ± 1.1	1.6 ± 1.1	.8[a]
Viral decline rate ($\log_{10}$/day)				
First phase	2.1 ± 0.9	1.5 ± 0.6	0.7 ± 0.5	<.0001[a]
Second phase	0.05 ± 0.05	0.04 ± 0.02	0.006 ± 0.008	<.0001[a]

ALT, alanine aminotransferase; BMI, body mass index.
[a]*P* values were determined by Kruskal–Wallis test.
[b]*P* values were determined by chi-square test.
[c]Response to previous IFN treatment.

tion–associated gene 5 (MDA5) play essential roles in initiating the host antiviral response by detecting intracellular viral dsRNA.[9,10] Caspase-recruiting domain (CARD) adaptor inducing IFN-β (Cardif), also called IFN-β promoter stimulator 1 (IPS-1), mitochondrial antiviral signaling protein (MAVS), and virus-induced signaling adaptor (VISA), is an adaptor molecule. Cardif connects RIG-I sensing to downstream signaling, resulting in IFN-β gene activation.[11–14] On the other hand, RIG-I sensing has been shown to be negatively regulated in a dominant-negative manner by LGP2,[10,15] a helicase related to RIG-I and MDA5 lacking CARD. Interestingly, the ubiquitin ligase ring-finger protein 125 (RNF125) has been recently shown to conjugate ubiquitin to RIG-I, MDA5 as well as Cardif, which results in suppressing the functions of these proteins.[16] Furthermore, these molecules are conjugated (ISGylated) by IFN-stimulated gene 15 (ISG15), a ubiquitin-like protein,[17] and ISG15 is specifically removed from ISGylated protein by ubiquitin-specific protease 18 (USP18), also called ubiquitin-specific protease 43 (UBP43).[18,19] Moreover, the NS3/4A protease of HCV specifically cleaves Cardif as part of its immune evasion strategy.[11,20] Therefore, the RIG-I/Cardif system and its regulatory systems have essential key functions in the innate antiviral response (see Supplementary Figure 1 online at www.gastrojournal.org). However, the clinical significance of these innate immune systems, especially in relevance to the treatment response, is unclear because findings in this field have been mainly obtained by in vitro experiments using cell lines.

The aims of this study were to elucidate the mechanisms underlying resistance to antiviral therapy in the clinical setting and to determine whether quantification of transcripts of positive and negative cytoplasmic viral sensors and related regulatory molecules involving innate immune system is useful in predicting responses to PEG-IFN-α and ribavirin combination therapy.

Patients and Methods

Patients

Among patients with biopsy-proven chronic hepatitis C hospitalized at the Musashino Red Cross Hospital, 74 patients of HCV genotype 1b with a high viral load (>100,000 IU/mL by Amplicor-HCV Monitor Assay; Roche Molecular Diagnostics Co, Tokyo, Japan) were included in the present study (Table 1). Patients with cirrhosis, autoimmune hepatitis, or alcoholic liver injury were excluded. No patient was positive for hepatitis B virus–associated antigen/antibody or anti- human immunodeficiency virus antibody. No patient received immunomodulatory therapy prior to the enrollment. Written informed consent was obtained from all the patients, and this study was approved by the Ethical Committee of Musashino Red Cross Hospital in accordance with the Helsinki Declaration. Five patients with nonviral liver disease (2 had autoimmune hepatitis and 3 had primary biliary cirrhosis) were included in the present study as controls.

Treatment Protocol

The patients were treated for 48 weeks with subcutaneous injections of PEG-IFN-α-2b (PegIntron; Schering-Plough Corporation, Kenilworth, NJ) at a dose of 1.5 $\mu g \cdot kg^{-1} \cdot week^{-1}$. Ribavirin (Rebetol; Schering-Plough Corporation) was administered concomitantly over the 48-week period, given orally twice daily at a total daily dose of 600 mg for the patients who weighed less than 60 kg and 800 mg for the patients who weighed between 60 and 80 kg. The dose of PEG-IFN-α-2b was reduced to 0.75 $\mu g \cdot kg^{-1} \cdot week^{-1}$ when either the neutrophil count was $<750/mm^3$ or the platelet count was $<80 \times 10^3/mm^3$. The dose of ribavirin was reduced to 600 mg/day when the hemoglobin concentration decreased to <10 g/dL.

Measurement of Gene Expression in the Liver

Liver biopsy was performed immediately before starting the therapy. After extraction of total RNA from liver biopsy specimens, the messenger RNA (mRNA) expression of positive and negative cytoplasmic viral sensors (RIG-I, MDA5, and LGP2), the adaptor molecule (Cardif), related ubiquitin E3-ligase (RNF125), and the modulators of these molecules (ISG15 and USP18) was quantified by real-time quantitative polymerase chain reaction (PCR) using primers specific for target genes. In brief, total RNA was extracted by the acid-guanidinium-phenol-chloroform method using Isogen (Nippon Gene Co Ltd, Toyama, Japan) from the liver biopsy specimen, which was 0.2–0.4 cm in length and 13 gauge in diameter. Complementary DNA (cDNA) was transcribed from 2 μg total RNA template in a 140-μL reaction mixture using a SYBR RT-PCR Kit (Takara Bio Co Ltd, Otsu, Japan) with random hexamer. Real-time quantitative PCR was performed using Smart Cycler version II (Takara Bio Co Ltd) with the SYBR RT-PCR Kit (Takara Bio Co Ltd) according to the manufacturer's instructions, and intercalating SYBR Green I (Molecular Probes Inc, Eugene, Oregon) was detected. Assays were performed in duplicate, and the expression levels of target genes were normalized to expression of the glyceraldehyde-3-phosphate dehydrogenase (G3PDH) gene and hydroxymethylbilane synthase, which is stable in the liver, as quantified using real-time quantitative PCR as internal controls. For accurate normalization, a set of 2 housekeeping genes was used in the present study. Sequences of primer sets were as follows: RIG-I: 5′-AAAGCATGCATGGTGTTCCAGA-3′, 5′-TCATTCGTGCATGCTCACTGATAA-3′; MDA5: 5′-ACATAACAGCAACATGGGCAGTG-3′, 5′-TTTGGTAAGGCCTGAGCTGGAG-3′; LGP2: 5′-ACAGCCTTGCAAACAGTACAACCTC-3′, 5′-GTCCCAAATTTCCGGCTCAAC-3′; Cardif: 5′-GGTGCCATCCAAAGTGCCTACTA-3′, 5′-CAGCACGCCAGGCTTACTCA-3′; RNF125: 5′-AGGGCACATATTCGGACTTGTCA-3′, 5′-CGGGTATTAAACGGCAAAGTGG-3′; ISG15: 5′-AGCGAACTCATCTTTGCCAGTACA-3′, 5′-CAGCTCTGACACCGACATGGA-3′; USP18: 5′-TGGTTCTGCTTCAATGACTCCAATA-3′, 5′-TTTGGGCATTTCCATTAGCACTC-3′; GAPDH: 5′-GCACCGTCAAGGCTGAGAAC-3′, 5′-TGGTGGTGAAGACGCCAGT-3′. hydroxymethylbilane synthase: 5′-AAGCGGAGCCATGTCTGGTAAC-3′, 5′-GTACCCACGCGAATCACTCTCA-3′.

Sequential Measurement of Gene Expression in Peripheral Blood Mononuclear Cells Before and During Therapy

To understand transcriptional response of the genes to PEG-IFN-α-2b and ribavirin therapy, serial expression of RIG-I, RNF125, Cardif, ISG15, and USP18 were determined before and during treatment in peripheral blood mononuclear cells (PBMC) in 14 patients (7 were sustained viral responders [SVR] and 7 were NVR). PBMC was obtained from whole blood samples collected before and at 4, 8, 24, 48, and 168 hours after the initiation of PEG-IFN-α-2b and ribavirin combination therapy. After extraction of total RNA from the PBMC, the expression of mRNA was quantified at each specified time point using real-time quantitative PCR as described above. Gene expression levels at each time point during treatment were calculated relative to baseline expression levels measured prior to IFN treatment.

Western Blotting

Western blotting was carried out in 9 patients (5 were SVR and 4 were NVR) and 3 non-HCV control subjects as described previously.[21] Liver biopsy specimen of ~10 mg was homogenized in 100 μL Complete Lysis-M (Roche Applied Science, Penzberg, Germany). Twenty micrograms of the homogenates were separated by SDS-PAGE and blotted onto a polyvinylidene difluoride Western blotting membrane. The membrane was incubated with the primary antibodies followed by a peroxidase-labeled anti-IgG antibody and visualized by chemiluminescence using the ECL Western blotting Analysis System (Amersham Biosciences, Buckinghamshire, United Kingdom). The anti-VISA mouse monoclonal antibody (BioDesign, Saco, ME) and anti-β-actin antibody (Sigma Chemical Co, St. Louis, MO) were used.

HCV Dynamics in Serum

To analyze the viral dynamics, HCV RNA was quantified just before and at 4, 8, and 24 hours and 2, 7, 14, 28, 56, and 84 days after the initiation of PEG-IFN-α-2b and ribavirin combination therapy, using real-time detection PCR, as reported previously.[22] For each patient, the viral decline curve was plotted on a semilogarithmic scale, and the slopes of the exponential viral declines were calculated for each viral decline phase with a straight-line fit of the data.

Definitions of Response to Therapy

A patient negative for serum HCV RNA during the first 6 months after the completion of PEG-IFN-α-2b and ribavirin combination therapy was defined as an SVR, and a patient for whom HCV RNA became negative at the end of therapy and reappeared after completion of therapy was defined as a transient responder (TR). A patient who was positive for HCV RNA even during the course of therapy was defined as an NVR. HCV RNA was determined with the Amplicor qualitative assay (Roche Molecular Diagnostics Co, Tokyo, Japan). The detection sensitivity of this assay is approximately 50 IU/mL.

Statistical Analysis

Categorical data were compared by the χ^2 test and Fisher exact test. Distributions of continuous variables were analyzed by Mann–Whitney U test for 2 groups. Kruskal–Wallis test was used for multiple group comparisons. All tests of significance were 2-tailed, and P values $< .05$ were considered statistically significant.

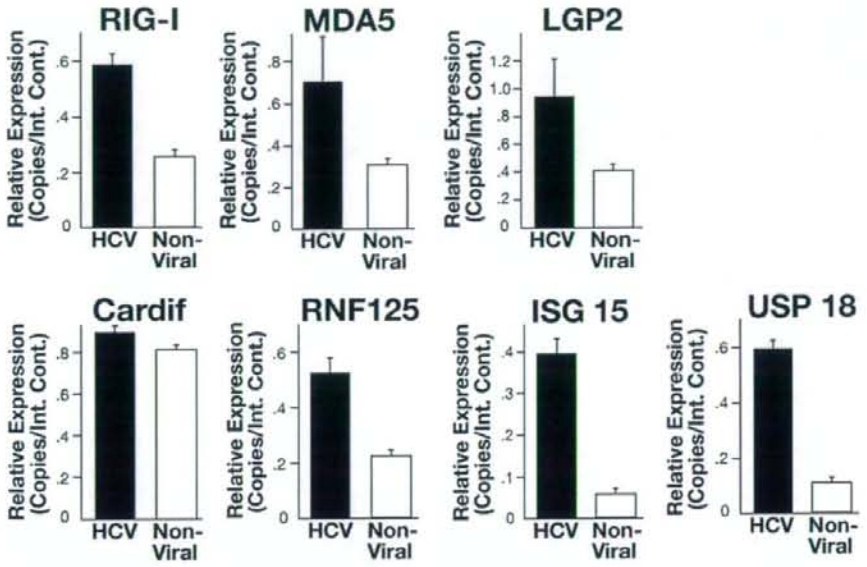

Figure 1. Comparison of hepatic gene expression levels between chronic hepatitis C patients (n = 74) and nonviral liver disease patients (n = 5). Expression levels of RIG-I, MDA5, LGP2, Cardif, RNF125, ISG15, and USP18 are shown. *Error bars* indicate the standard error. Upon HCV infection, expression of these genes except Cardif was stimulated. The *P* values determined by Mann–Whitney *U* test between 2 groups were as follows: RIG-I, *P* .02; MDA5, *P* .01; LGP2, *P* .005; Cardif, *P* .7; RNF125, *P* .06; ISG15, *P* .007; USP18, *P* .004.

Results

Patient Characteristics

According to the final virologic response, patients were classified into 3 groups: 30 were SVR, 24 were TR, and the remaining 20 were NVR, as shown in Table 1. Viral decline rates in NVR were significantly lower in both the first and second phases of HCV dynamics. It should be noted that most NVR patients exhibited no second-phase viral decline.

Data on factors that were available before starting the treatment were compared according to virologic response by univariate analysis. As shown in Table 1, only age and platelet count were associated with viral response, and no other clinical factors were predictive of NVR before initiation of the therapy.

Gene Expression Involving Innate Immunity in the Liver

First, we compared basal hepatic gene expression between the chronic hepatitis C patients (n = 74) and the nonviral liver disease patients (n = 5). As shown in Figure 1, levels of RIG-I, MDA5, LGP2, ISG15, and USP18 expression were significantly higher in the chronic hepatitis C patients than in the nonviral liver disease patients. However, there was no significant difference in levels of Cardif expression between the chronic hepatitis C and nonviral-related liver disease patients.

Next, to assess the relationship between baseline hepatic gene expression and treatment efficacy, levels of gene expression were compared based on the final virologic response. As shown in Figure 2, the hepatic expression levels of RIG-I, MDA5, and LGP2 were significantly higher in NVR than in SVR and TR. In marked contrast, hepatic Cardif expression was significantly lower in the NVR group. The hepatic expression of RNF125, which is specific E3-ubiquitin ligase for RIG-I, MDA5, and Cardif, was also significantly lower in the NVR group. Because negative correlation was found between RIG-I and Cardif or RNF125 expression, we calculated the ratio of RIG-I to Cardif or RNF125 expression levels. As shown in Figure 2, the difference among the groups was conspicuous when comparison was made with the RIG-I/Cardif ratio or RIG-I/RNF125 ratio. Moreover, the RIG-I/Cardif expression ratio before treatment was negatively and significantly correlated with the exponential viral decline rate in both the first and the second phases of HCV dynamics (first phase, $r = -0.4$, $P < .0005$; second phase, $r = -0.5$, $P < .0001$). Similar correlation was found between RIG-I/RNF125 ratio and viral decline rate (first phase, $r = -0.4$, $P = .004$; second phase, $r = -0.2$, $P = .09$, data not shown).

Like RIG-I and MDA5, intrahepatic expression levels of ISG15 and USP18 were significantly higher in NVR than in SVR and TR (Figure 2). When we assessed the correlation of these 2 genes in individual patients, we found a strong and significant correlation between ISG15 and USP18 ($r^2 = 0.88$, $P < .0001$). Levels of ISG15 and USP18 expression before treatment were negatively correlated with the exponential viral decline rates calculated from

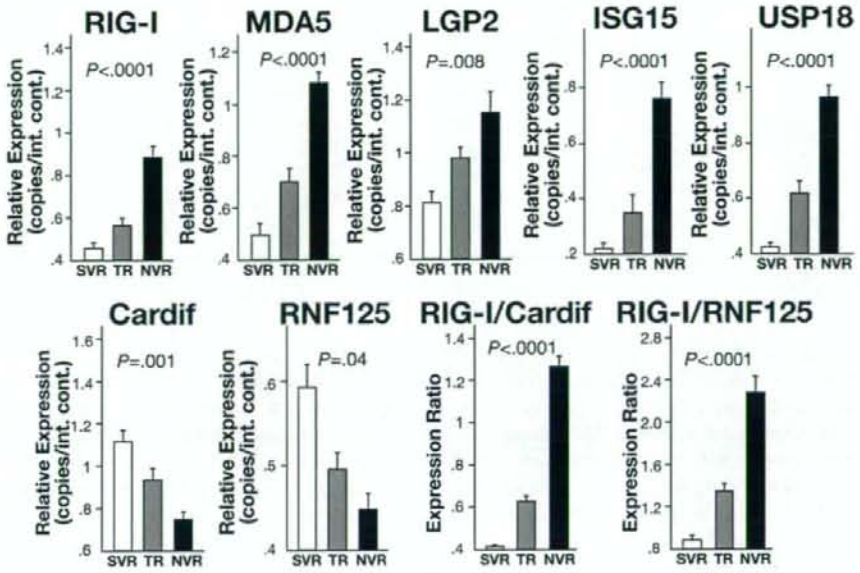

Figure 2. Comparison of hepatic gene expression levels according to final virologic outcome. Expression levels of RIG-I, MDA5, LGP2, ISG15, USP18, Cardif, RNF125, RIG-I/Cardif ratio, and RIG-I/RNF125 ratio are shown. *Open columns* indicate SVR (n = 30), *shaded columns* indicate TR (n = 24), and *solid columns* indicate NVR (n = 20). *Error bars* indicate the standard error. The *P* values were analyzed by the Kruskal–Wallis test.

the first and the second phases of HCV dynamics (ISG15, first phase, $r = -0.5$, $P < .0001$; ISG15, second phase, $r = -0.3$, $P = .02$; USP18, first phase, $r = -0.5$, $P < .0001$; USP18, second phase, $r = -0.3$, $P = .01$).

Receiver Operator Characteristic Analysis

To determine the usefulness of these gene quantifications as predictors, receiver operator characteristic (ROC) analysis was conducted (Figure 3). The area under the ROC curve for the RIG-I/Cardif ratio, ISG15, and USP18 was 0.91, 0.90, and 0.91, respectively, suggesting that quantification of these gene transcripts is of use for the prediction of NVR (Table 2). In addition, this analysis also suggested that RIG-I/Cardif ratio would be more specific for prediction of NVR, whereas ISG15 and USP18 would be more sensitive (Table 2).

Multivariate Analysis

Multivariate analysis for factors that were available before initiating therapy indicated that a higher ratio of RIG-I/Cardif and higher expression of ISG15 were independent factors that were associated with NVR (Table 3). In this analysis, USP18 was excluded because of its strong correlation with ISG15.

Protein Levels of Cardif in the Liver

Because hepatic expression of Cardif mRNA was significantly lower in NVR patients than in SVR patients,

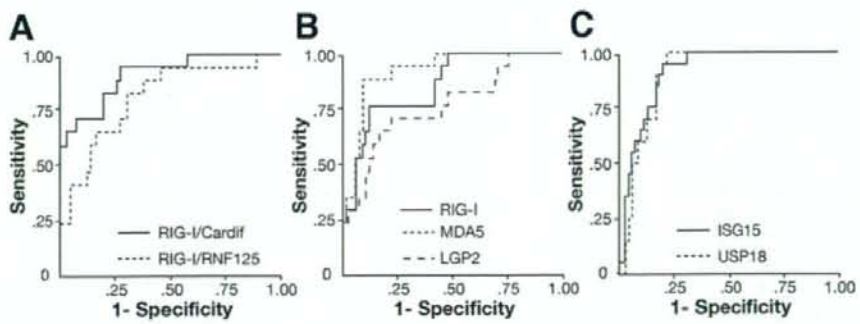

Figure 3. Receiver operator characteristic (ROC) curve for prediction of nonvirologic response. ROC curves were generated to compare (*A*) RIG-I/Cardif ratio (*solid line*) and RIG-I/RNF125 ratio (*shaded line*); (*B*) RIG-I (*solid line*), MDA5 (*shaded line*), and LGP2 (*dotted line*); and (*C*) ISG15 (*solid line*) and USP18 (*shaded line*).

Table 2. Area Under the ROC Curves, Sensitivity, Specificity, and Negative and Positive Predictive Values of Non-Virologic Responses

Variables	Az	95% CI	Cut-off	Sensitivity	Specificity	NPV[a]	PPV[b]
RIG-I	0.89	0.78–0.95	0.68	0.80	0.87	0.92	0.70
MDA5	0.92	0.86–0.98	0.84	0.82	0.89	0.93	0.74
LGP2	0.76	0.63–0.90	1.03	0.65	0.72	0.85	0.46
RIG-I/Cardif	0.91	0.84–0.99	0.88	0.75	0.91	0.91	0.75
RIG-I/RNF125	0.81	0.69–0.93	1.05	0.82	0.62	0.91	0.43
ISG15	0.91	0.85–0.97	0.36	0.90	0.81	0.96	0.64
USP18	0.90	0.84–0.96	0.67	0.90	0.83	0.96	0.67

[a]NPV, negative predictive value.
[b]PPV, positive predictive value.

we determined the basal protein expression levels of Cardif in the liver in NVR and SVR patients. Western blot analysis demonstrated a single Cardif product in all samples (Figure 4*A*). Similar to Cardif mRNA expression, mean Cardif expression in NVR patients was significantly lower than that in SVR (Figure 4*B*, $P = .01$). The cleavage product of Cardif, which has been reported by Loo et al,[23] was not detected in our analyses.

Transcriptional Responses to PEG-IFN-α-2b and Ribavirin Therapy in PBMC

Sequential analysis in response to PEG-IFN-α-2b and ribavirin demonstrated a rapid and strong induction of RIG-I, ISG15, and USP18 mRNA expression, which peaked 8 hours after PEG-IFN-α-2b administration (Figure 5). A greater fold change of these peak inductions was observed in SVR patients compared with NVR patients, although statistical significance was not achieved. In marked contrast, RNF125 expression profile in response to PEG-IFN-α-2b was triphasic, and consisted of (1) rapid and strong suppression peaked at 8 hours after administration, (2) increased 1.5- to 2-fold above baseline level during 24–48 hours after the administration, and (3) gradually decreased to baseline level (Figure 5). The rapid suppression and subsequent increase following PEG-IFN-α-2b administration tended to have a greater fold change in NVR patients compared with those in SVR patients. In contrast from RIG-I, ISG15, USP18, and RNF125, Cardif expression profile was relatively constitutive, and transcriptional response to PEG-IFN was weak (Figure 5).

Discussion

In the present study, we found that baseline expression levels of intrahepatic viral sensors and related regulatory molecules were significantly associated with the final virologic outcome in patients with chronic hepatitis C who were treated with PEG-IFN-α-2b and ribavirin combination therapy: up-regulation of RIG-I, MDA5, LGP2, ISG15, and USP18 and lower expression of Cardif and RNF125 could predict nonresponse to subsequent treatment with PEG-IFN-α-2b and ribavirin. The positive predictive value of a high ratio of expression of RIG-I to Cardif (>0.88) for NVR was the highest at a value of 0.75, and the negative predictive values of high expression of ISG15 (>0.36/internal control) and USP18 (>0.67/internal control) were the highest at values of both 0.96. These data may be of use in predicting clinical responses to the PEG-IFN-α and ribavirin combination before initiating therapy.

Table 3. Multivariate Analysis for the Factors Associated With Non-Virologic Response

Variable	Odds ratio	95% CI	*P* value
RIG-I/Cardif Ratio (by 0.1)	1.5	1.1–2.1	.008
RIG-I/RNF125 Ratio (by 0.1)	1.2	1.0–2.5	.1
ISG15 (by 0.1/internal control)	1.5	1.1–2.0	.01
Age (by 1 y)	1.0	0.9–1.1	.6
Platelet count (by $1 \times 10^4/\mu L$)	1.2	0.9–1.5	.07

Previously, large randomized controlled trials identified several pretreatment factors associated with the final virologic outcome, such as genotype, HCV RNA level, degree of fibrosis, age, body weight, ethnicity, and steatosis.[24] However, these findings lead us to believe that predicting the final virologic response before initiating PEG-IFN-α and ribavirin is difficult. Indeed, only age and platelet count were associated with the outcome in our patients with genotype 1b and a high viral load. Currently, the final response can be gauged only after treatment has been initiated. Although an early viral response at 12 weeks suggests the eventual outcome with 60%–90% accuracy,[25] a 12-week regimen is associated with adverse effects and is expensive. Therefore, this study investigated the baseline expression of genes involving innate immunity that may have significant effects on clinical outcomes.

In the present study, we demonstrated that RIG-I and MDA5 were inducible upon HCV infection and that expression of these intrahepatic positive viral sensors was up-regulated in NVR. In vitro studies have suggested that RIG-I and MDA5 play a pivotal role in the regulation of IFN production and augment the production of IFN via an amplification circuit. These results suggest that expression of RIG-I and MDA5 and related amplification system may be up-regulated by endogenous IFN at a higher baseline level in NVR patients. However, HCV elimination by subsequent exogenous IFN is insufficient

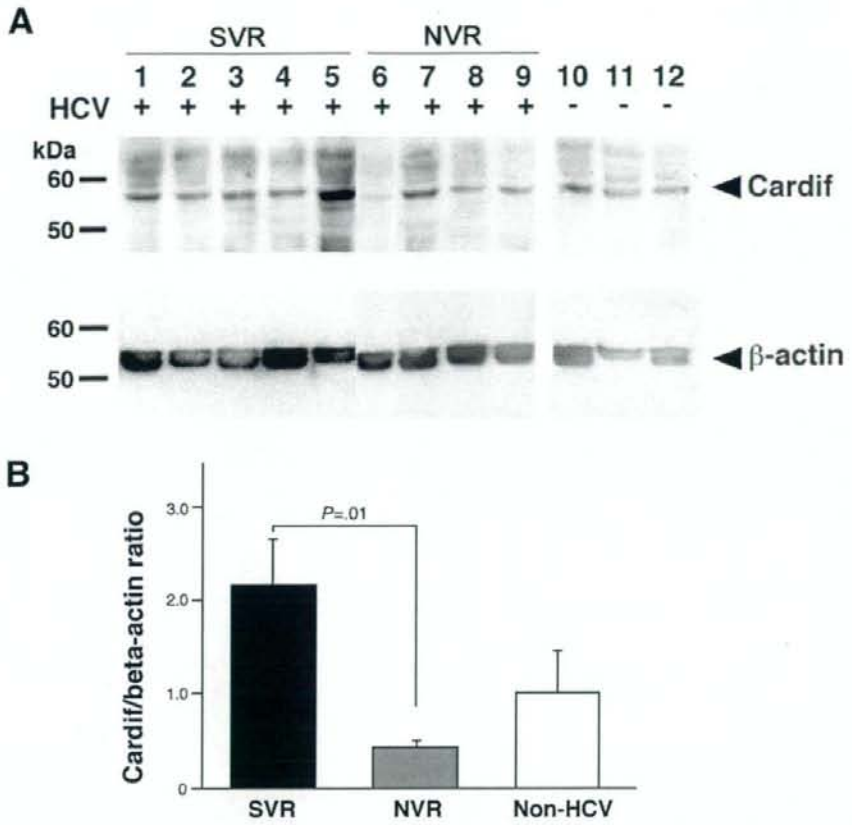

Figure 4. (*A*) Western blot analysis. Five lanes were SVR (*lanes 1–5*), 4 lanes were NVR (*lanes 6–9*), and 3 lanes were non-HCV control (*lanes 10–12*). Specific bands for Cardif and β-actin are indicated by *arrows*. (*B*) Expression level of Cardif protein normalized to β-actin in the liver biopsy specimens according to ultimate treatment response. *Error bars* indicate the standard error.

in these patients, suggesting that NVR patients may have adopted a different equilibrium in their immune response to the virus. In contrast to the expression of RIG-I and MDA5, Cardif mRNA, which was expressed in a relatively constitutive fashion, was significantly lower in NVR. Our ROC analysis highlights that lower expression of Cardif relative to that of RIG-I was one of the strongest predictors for NVR. Moreover, Western blot analysis further confirmed the down-regulation of Cardif in NVR patients, as demonstrated by its protein level. Because Cardif is one of the substantial target molecules of HCV evasion,[11,20] it is likely that Cardif expression is suppressed by HCV with resistant phenotype or is inadequate in NVR patients. Loo et al have demonstrated a Cardif cleavage product in 2 of 4 liver tissue samples of chronic HCV infection.[23] In our study, however, the Cardif cleavage product was not detected, presumably because the product could be unstable in vivo, resulting in rapid degradation. Although further studies are necessary to elucidate mechanisms of Cardif down-regulation, our findings of lower expression of Cardif in NVR suggested that the status of Cardif expression in the liver might have a significant effect on the ultimate outcome of antiviral treatment.

The antiviral effect brought by RIG-I/Cardif signaling is regulated by the coordination of negative and positive regulators. It has been shown that RNF125 functions as a negative regulator of RIG-I/Cardif signaling. RNF125 is an ubiquitin E3-ligase with activity against protein containing CARD domains, such as RIG-I, MDA5, and Cardif, and these ubiquitinated molecules undergo proteasomal degradation. In contrast, RNF125 do not have negative function against LGP2, a negative regulator of RIG-I signaling, because LGP2 lacks CARD domain. In contrast to RIG-I, RNF125 expression was rapidly suppressed by exogenous IFN; therefore, observed lower basal hepatic level of RNF125 in NVR could be explained by the suppressive effect of endogenous IFN, which may be up-regulated in NVR patients. Hence, RNF125 may constitute a negative regulatory circuit for IFN production and is responsible for responsiveness to PEG-IFN and ribavirin therapy.

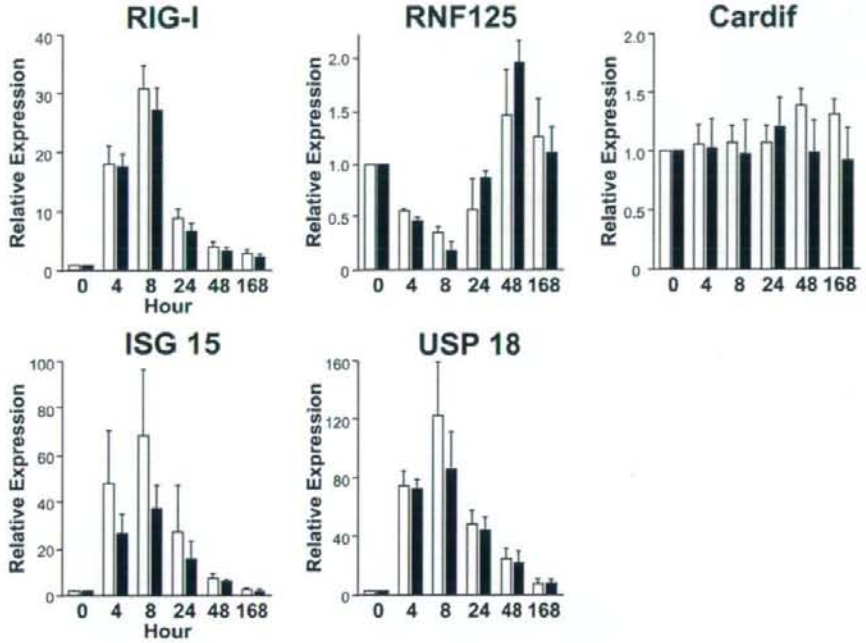

Figure 5. Transcriptional responses during PEG-IFN-α-2b and ribavirin therapy in PBMC (n = 14). *Open columns* indicate SVR (n = 7), and *solid columns* indicate NVR (n = 7). *Error bars* indicate the standard error. The *P* values determined by Mann–Whitney *U* test between 2 groups at 8 hours were as follows: RIG-I, *P* .3; RNF125, *P* .3; Cardif, *P* .7; ISG15, *P* .3; USP18, *P* .2.

It has been shown that RIG-I function is modified by ISG15 via ISGylation.[17] Consistent with our data, Chen et al identified 18 genes, including ISG15 and USP18, whose expression differed between responders and nonresponders.[26] Interestingly, a recent study has shown that USP18 negatively regulates IFN signaling independently of its isopeptidase activity toward ISG15 by binding to the IFNAR2 receptor subunit and blocking the interaction between Janus kinase and the IFN receptor.[27] Moreover, the siRNA knockdown of USP18 in human cells has consistently been shown to potentiate the ability of IFN to inhibit HCV RNA replication.[28] Therefore, USP18 is suggested as a novel in vivo inhibitor of signal transduction pathways that are specifically triggered by type I IFN. Consistent with a role for USP18 in down-regulating the antiviral IFN response, we confirmed that up-regulation of USP18 was one of the factors predicting a lack of response to treatment with IFN.

The mechanism underlying the association of gene expression involving innate immunity with resistance to therapy is not well understood. Our human study with HCV patients treated by PEG-IFN and ribavirin highlights RIG-I/Cardif, RIG-I/RNF125, and ISG15/USP18, which is partly responsible for the clinical responsiveness to antiviral therapy. RIG-I signaling by viral pathogens may affect a wide variety of responses in not only innate but also acquired immunity. Our study is the first to demonstrate the potential relevance between molecules involving innate immunity and the clinical response to antiviral therapy.

In addition, sequential analysis of expression profile during PEG-IFN-α-2b and ribavirin treatment was also performed in this study. Lanford et al demonstrated transcriptional response to IFN-α in chimpanzee by genome microarray analysis, which included RIG-I, ISG15, and USP18.[29] An association of transcriptional response with early phase of virologic response has been also reported in PBMC or liver biopsy specimen.[30-32] We recently reported that the transcriptional double-stranded RNA-activated protein kinase response during treatment with PEG-IFN-α-2b and ribavirin was associated with the ultimate clinical response.[30] Similarly, the present study demonstrated a strong and rapid increase of RIG-I, ISG15, and USP18 mRNA in response to clinical PEG-IFN treatment especially in SVR patients, although few patients were available to achieve statistical significance between SVR and NVR. In marked contrast, transcriptional response of RNF125 exhibited a triphasic pattern. Rapid suppression seen in the first phase was presumably because of a negative regulatory effect of IFN. However, increase of RNF125 mRNA in the second phase, which tended to be grater in NVR, may be responsible for inhibiting RIG-I expression seen 8–48 hours after PEG-IFN-α-2b administration. Although limitations includ-

ing the use of PBMC and small sample size still deserve mention, the sequential expression profile during treatment may provide further valuable information regarding the prediction of the clinical response to the therapy and the mechanism of action of antiviral treatment.

In the present study, we have included patients with genotype 1b because it is imperative to designate a virologically homogeneous patient group to associate individual treatment responses with different gene expression profiles that direct innate immune responses. We have preliminarily studied genotype 2 patients and found that Cardif and RNF125 gene expression levels in NVR patients were significantly lower than those with SVR patients ($P = .03$ and $P = .04$, respectively) and that RIG-I/Cardif and RIG-I/RNF125 ratios were significantly higher in NVR patients ($P = .02$ and $P = .009$, respectively, see Supplementary Figure 2 online at www.gastrojournal.org). These findings suggest that the differences in gene expression profiles between SVR and NVR were almost identical to those demonstrated in patients with genotype 1b. However, the correlation between treatment responses in all the genotypes and the different status of innate immune responses needs to be explored. Further studies may be necessary to clarify this issue.

In conclusion, the results of the present study offer potentially important clinical implications for patients with chronic hepatitis C who are treated with PEG-IFN-α and ribavirin. Quantifying hepatic gene expression of the RIG-I/Cardif system, including its regulators before treatment, is useful in identifying patients who are at a higher risk for NVR. The data from these assays can provide valuable information that may influence the decision about the treatment strategy in each individual patient. Finally, this clinical human study demonstrates the potential relevance of the molecules involving innate immunity to the clinical response to therapy. Our data will help understand the pathogenesis of HCV resistance and development of new antiviral therapy targeted toward the innate immune system.

Supplementary Data

Note: To access the supplementary material accompanying this article, visit the online version of *Gastroenterology* at www.gastrojournal.org, and at doi: 10.1053/j.gastro.2008.02.019.

References

1. Kiyosawa K, Sodeyama T, Tanaka E, et al. Interrelationship of blood transfusion, non-A, non-B hepatitis and hepatocellular carcinoma: analysis by detection of antibody to hepatitis C virus. Hepatology 1990;12:671–675.
2. Manns MP, McHutchison JG, Gordon SC, et al. Peginterferon alfa-2b plus ribavirin compared with interferon alfa-2b plus ribavirin for initial treatment of chronic hepatitis C: a randomised trial. Lancet 2001;358:958–965.
3. Fried MW, Shiffman ML, Reddy KR, et al. Peginterferon alfa-2a plus ribavirin for chronic hepatitis C virus infection. N Engl J Med 2002;347:975–982.
4. Hadziyannis SJ, Sette HJ, Morgan TR, et al. PEGASYS International January 2006 American Gastroenterological Association 253 Study Group. Peginterferon-α-2a and ribavirin combination therapy in chronic hepatitis C: a randomized study of treatment duration and ribavirin dose. Ann Intern Med 2004;140:346–355.
5. Zeuzem S, Pawlotsky JM, Lukasiewicz E, et al. DITTO-HCV Study Group. International, multicenter, randomized, controlled study comparing dynamically individualized versus standard treatment in patients with chronic hepatitis C. J Hepatol 2005;43:250–257.
6. Berg T, von Wagner M, Nasser S, et al. Extended treatment duration for hepatitis C virus type 1: comparing 48 versus 72 weeks of peginterferon-alfa-2a plus ribavirin. Gastroenterology 2006;130:1086–1097.
7. Biron CA. Initial and innate responses to viral infections—pattern setting in immunity or disease. Curr Opin Microbiol 1999;2:374–381.
8. Gale M Jr, Foy EM. Evasion of intracellular host defence by hepatitis C virus. Nature 2005;436:939–945.
9. Yoneyama M, Kikuchi M, Natsukawa T, et al. The RNA helicase RIG-I has an essential function in double-stranded RNA-induced innate antiviral responses. Nat Immunol 2004;5:730–737.
10. Yoneyama M, Kikuchi M, Matsumoto K, et al. Shared and unique functions of the DExD/H-box helicases RIG-I, MDA5, and LGP2 in antiviral innate immunity. J Immunol 2005;175:2851–2858.
11. Meylan E, Curran J, Hofmann K, et al. Cardif is an adaptor protein in the RIG-I antiviral pathway and is targeted by hepatitis C virus. Nature 2005;437:1167–1172.
12. Kawai T, Takahashi K, Sato S, et al. IPS-1, an adaptor triggering RIG-I- and Mda5-mediated type I interferon induction. Nat Immunol 2005;6:981–988.
13. Seth RB, Sun L, Ea CK, et al. Identification and characterization of MAVS, a mitochondrial antiviral signaling protein that activates NF-κB and IRF 3. Cell 2005;122:669–682.
14. Xu LG, Wang YY, Han KJ, et al. VISA is an adapter protein required for virus-triggered IFN-β signaling. Mol Cell 2005;19:727–740.
15. Rothenfusser S, Goutagny N, DiPerna G, et al. The RNA helicase Lgp2 inhibits TLR-independent sensing of viral replication by retinoic acid-inducible gene-I. J Immunol 2005;175:5260–5268.
16. Arimoto K, Takahashi H, Hishiki T, et al. Negative regulation of the RIG-I signaling by the ubiquitin ligase RNF125. Proc Natl Acad Sci U S A 2007;104:7500–7505.
17. Zhao C, Denison C, Huibregtse JM, et al. Human ISG15 conjugation targets both IFN-induced and constitutively expressed proteins functioning in diverse cellular pathways. Proc Natl Acad Sci U S A 2005;102:10200–10205.
18. Schwer H, Liu LQ, Zhou L, et al. Cloning and characterization of a novel human ubiquitin-specific protease, a homologue of murine UBP43 (Usp18). Genomics 2000;65:44–52.
19. Malakhov MP, Malakhova OA, Kim KI, et al. UBP43 (USP18) specifically removes ISG15 from conjugated proteins. J Biol Chem 2002;277:9976–9981.
20. Li XD, Sun L, Seth RB, et al. Hepatitis C virus protease NS3/4A cleaves mitochondrial antiviral signaling protein off the mitochondria to evade innate immunity. Proc Natl Acad Sci U S A 2005;102:17717–17722.
21. Nakagawa M, Sakamoto N, Tanabe Y, et al. Suppression of hepatitis C virus replication by cyclosporin A is mediated by blockade of cyclophilins. Gastroenterology 2005;129:1031–1041.
22. Asahina Y, Izumi N, Uchihara M, et al. A potent antiviral effect on hepatitis C viral dynamics in serum and peripheral blood mononuclear cells during combination therapy with high-dose daily

interferon α plus ribavirin and intravenous twice-daily treatment with interferon β. Hepatology 2001;34:377–384.
23. Loo YM, Owen DM, Li K, et al. Viral and therapeutic control of IFN-β promoter stimulator 1 during hepatitis C virus infection. Proc Natl Acad Sci U S A 2006;103:6001–6006.
24. Dienstag JL, McHutchison JG. American Gastroenterological Association technical review on the management of hepatitis C. Gastroenterology 2006;130:231–264.
25. National Institutes of Health. National Institutes of Health Consensus Development Statement: management of hepatitis. Hepatology 2002;36(Suppl 1):S3–S20.
26. Chen L, Borozan I, Feld J, et al. Hepatic gene expression discriminates responders and nonresponders in treatment of chronic hepatitis C viral infection. Gastroenterology 2005;128:1437–1444.
27. Malakhova OA, Kim KI, Luo JK, et al. UBP43 is a novel regulator of interferon signaling independent of its ISG15 isopeptidase activity. EMBO J 2006;25:2358–2367.
28. Randall G, Chen L, Panis M, et al. Silencing of USP18 potentiates the antiviral activity of interferon against hepatitis C virus infection. Gastroenterology 2006;131:1584–1591.
29. Lanford RE, Guerra B, Lee H, et al. Genomic response to interferon-α in chimpanzees: implications of rapid down-regulation for hepatitis C kinetics. Hepatology 2006;43:961–972.
30. Asahina Y, Izumi N, Umeda N, et al. Pharmacokinetics and enhanced PKR response in patients with chronic hepatitis C treated with pegylated interferon α-2b and ribavirin. J Viral Hepat 2007;14:396–403.
31. Taylor MW, Tsukahara T, Brodsky L, et al. Changes in gene expression during pegylated interferon and ribavirin therapy of chronic hepatitis C virus distinguish responders from nonresponders to antiviral therapy. J Virol 2007;81:3391–3401.
32. Feld JJ, Nanda S, Huang Y, et al. Hepatic gene expression during treatment with peginterferon and ribavirin: identifying molecular pathways for treatment response. Hepatology 2007;46:1548–1563.

Received August 30, 2007. Accepted January 31, 2008.

Address requests for reprints to: Namiki Izumi, MD, PhD, Chief, Department of Gastroenterology and Hepatology, Musashino Red Cross Hospital, 1-26-1 Kyonan-cho, Musashino-shi, Tokyo 180-8610, Japan. e-mail: nizumi@musashino.jrc.or.jp; fax: (81) 422-32-9551.

Supported by grants from the Miyakawa Memorial Research Foundation; the Japanese Ministry of Education, Culture, Sports, Science and Technology; and the Japanese Ministry of Welfare, Health and Labor.

Financial disclosures: The authors who participated in this study have had no affiliation with the manufacturers of the drugs involved either in the past or in present and have not received funding from the manufacturers to conduct this research.

 DOI 10.1002/eji.200838359 Eur. J. Immunol. 2008. 38: 3290–3303

European Journal of Immunology

FTY720 suppresses the development of colitis in lymphoid-null mice by modulating the trafficking of colitogenic CD4$^+$ T cells in bone marrow

Toshimitsu Fujii, Takayuki Tomita*, Takanori Kanai, Yasuhiro Nemoto, Teruji Totsuka, Naoya Sakamoto, Tetsuya Nakamura, Kiichiro Tsuchiya, Ryuichi Okamoto and Mamoru Watanabe*

Department of Gastroenterology and Hepatology, Graduate School, Tokyo Medical and Dental University, Tokyo, Japan

2-Amino-2-(2-[4-octylphenyl]ethyl)-1,3-propanediol hydrochloride (FTY720) suppresses T-cell egress from LN, thereby preventing pathogenic T cells from migrating toward disease sites. However, little is known about whether FTY720 could control the trafficking of T cells without the presence of lymphoid tissues. Here we demonstrate that FTY720 treatment suppresses the recirculation of CD4$^+$ T cells in splenectomized (SPX) lymphotoxin-$\alpha^{-/-}$ (LT-$\alpha^{-/-}$) mice that lack LN and spleen, as shown by peripheral blood (PB) lymphopenia in FTY720-treated SPX LT-$\alpha^{-/-}$ mice. In a short-term transfer experiment, the cell number of transferred Ly5.1$^+$CD4$^+$ T cells recovered from host FTY720-treated SPX LT-$\alpha^{-/-}$ mice (Ly5.2$^+$) was markedly decreased in PB, but conversely increased in BM. Notably, FTY720 treatment prevented the development of colitis that is otherwise induced in untreated SPX LT-$\alpha^{-/-}$ × RAG-2$^{-/-}$ mice upon transfer of colitic lamina propria CD4$^+$ T cells. In such mice, the number of CD4$^+$ T cells in PB or lamina propria of FTY720-treated SPX LT-$\alpha^{-/-}$ × RAG-2$^{-/-}$ recipients was significantly reduced, but that in the BM was significantly increased as compared with untreated control mice. Altogether, the present results indicate that FTY720 treatment may offer an additional role to direct trafficking of CD4$^+$ T cells in BM, resulting in the prevention of colitis.

Key words: Chronic colitis · Colitogenic CD4$^+$ T cells · FTY720 · Inflammatory bowel disease · Mucosal immunity

Supporting Information available online

Introduction

2-Amino-2-(2-[4-octylphenyl]ethyl)-1,3-propanediol hydrochloride (FTY720) is a sphingosine-1-phosphate (S1P) receptor modulator, which induces prolonged down-modulation of the surface expression of the S1P receptor and thereby inhibits the egress of lymphocytes from thymus, LN, and Peyer's patches leading to peripheral blood (PB) lymphopenia [1–8]. From the view of clinical application, in animal models, FTY720 has been shown to prevent autoimmune diseases [9, 10], viral infection [11, 12], or graft rejection after allotransplantation [13]. Moreover, it was recently shown that FTY720 reduced the number of lesions and clinical disease activity of patients with multiple sclerosis in a phase II, placebo-controlled trial [14].

In inflammatory bowel diseases (IBD), it is believed that colitogenic memory CD4$^+$ T cells are intermittently reactivated in

Correspondence: Dr. Takanori Kanai
e-mail: taka.gast@tmd.ac.jp

*These authors contributed equally to this work.

regional lymphoid organs in response to antigen-loading activated dendritic cells and thereafter return to inflammatory tissues [15–18]. We recently reported that colitogenic memory T cells survive for a long period in IL-7-dependent manner, by using a model of colitis induced by adoptive transfer of $CD4^+CD45RB^{high}$ T cells into SCID/RAG-deficient mice [19]. Although little was known about how colitogenic memory $CD4^+$ T cells in IBD are controlled by FTY720, we demonstrated that FTY720 suppresses the development of colitis induced by adoptive transfer of colitogenic lamina propria (LP) $CD4^+CD44^{high}CD62L^-$ effector-memory T (T_{EM}) cells [20, 21] that were obtained from colitic $CD4^+CD45RB^{high}$ T-cell-transferred SCID mice [22]. Furthermore, we found that FTY720 treatment induced marked lymphopenia of colitogenic $CD4^+$ T_{EM} cells in the periphery [22]. In this previous study, however, it was curious but very interesting as to why the colitogenic $CD4^+$ T_{EM} cells were controlled by FTY720 treatment, as they should preferentially reside in non-lymphoid tissues such as the gut [23, 24].

Thus, these previous results prompted us to investigate another possible effect of the FTY720 treatment, modulating a yet-known cell trafficking independent of the presence of LN and spleen. To this end, we here used splenectomized lymphotoxin-$\alpha^{-/-}$ (LT-$\alpha^{-/-}$) × RAG-$2^{-/-}$ mice lacking spleen, LN, and Payer's patches, as recipients for adoptive transfer of colitogenic $CD4^+$ T_{EM} cells and assessed the lymphoid tissue-independent effect of FTY720 treatment upon accumulation of donor T cells in the BM and prevention of colitogenic $CD4^+$ T_{EM} cell-mediated colitis.

Results

FTY720 induces lymphopenia in LT-$\alpha^{-/-}$ mice

To first assess the alterations of systemic T-cell number or its subset composition upon FTY720 treatment without an impact of lymphoid tissues including spleen, LN, and Peyer's patches, we used splenectomized (SPX) LT-$\alpha^{-/-}$ and the control SPX LT-$\alpha^{+/+}$ littermate mice in this study (Fig. 1A). Two weeks after splenectomy, mice were i.p. administered with a single dose of FTY720 (1.0 mg/kg) or control PBS, and then the tissue distribution of lymphocytes ($CD3^+CD4^+$, $CD3^+CD8^+$, and $CD19^+$cells) in the PB, LP, and BM at 24 h after administration was analyzed. The number of total $CD3^+CD4^+$ lymphocytes in the PB of FTY720-treated SPX LT-$\alpha^{+/+}$ mice was markedly decreased compared with that of PBS-treated SPX LT-$\alpha^{+/+}$ mice (Fig. 1B), suggesting a previously recognized LN-dependent mechanism of FTY720 that promotes the sequestration of lymphocytes and inhibits the egress of lymphocytes from LN [1–4]. Unlike the decreased number of $CD3^+CD4^+$ lymphocytes in the PB of FTY720-treated SPX LT-$\alpha^{+/+}$ mice, the difference in the number of those cells in LP or BM was not significant between FTY720- and PBS-treated SPX LT-$\alpha^{+/+}$ mice. In PBS-treated SPX LT-$\alpha^{-/-}$ mice, interestingly, the cell numbers of $CD3^+CD4^+$ lymphocytes in PB, LP, and BM were significantly increased compared with those in the paired PBS-treated SPX LT-$\alpha^{+/+}$ mice presumably due to the lack of LN serving as a reservoir of lymphocytes (Fig. 1B). Surprisingly, the cell number of $CD3^+CD4^+$ lymphocytes in the PB of FTY720-treated SPX LT-$\alpha^{-/-}$ mice was also significantly decreased compared with that of the paired PBS-treated SPX LT-$\alpha^{-/-}$ mice, suggesting an existence of as-yet-unknown reservoir for $CD3^+CD4^+$ lymphocytes other than LN or spleen (Fig. 1B). Moreover, although the number of $CD3^+CD4^+$ lymphocytes in the BM of SPX LT-$\alpha^{+/+}$ mice was not affected by FTY720 treatment, the number of such cells in the BM of FTY720-treated SPX LT-$\alpha^{-/-}$ mice was significantly increased compared with that of PBS-treated SPX LT-$\alpha^{-/-}$ mice. In contrast, the number of $CD3^+CD8^+$ T cells and $CD19^+$ B cells in the BM or in the LP was not affected by FTY720 treatment in any group of mice (Fig. 1B), whereas the number of those cells in the PB of FTY720-treated SPX LT-$\alpha^{+/+}$ and SPX LT-$\alpha^{-/-}$ mice was significantly decreased compared with that of the paired PBS-treated mice.

To further assess the possible effect of FTY720 on accumulation of $CD3^+CD4^+$ T cells within the BM of SPX LT-$\alpha^{-/-}$ mice, we next performed a short-term adoptive transfer of splenic $CD4^+$ T cells that were obtained from Ly5.1-derived C57BL/6J mice into Ly5.2-derived SPX LT-$\alpha^{-/-}$mice, by treating them with or without FTY720 at 3 h before transfer. Twenty-four hours after the transfer, mice were sacrificed, and the recovered cell number of the total and $Ly5.1^+$ $CD4^+$ donor cells at various sites was analyzed (Fig. 2A). Consistent with the above-mentioned results (Fig. 1), we confirmed that the number of $CD4^+$ T cells was significantly decreased in PB in FTY720-treated SPX LT-$\alpha^{-/-}$mice regardless of the host ($Ly5.2^+$) or donor ($Ly5.1^+$), but conversely, the number of those cells in the BM was significantly increased (Fig. 2B). Interestingly, the decreased cell number of $CD4^+$ T cells in the PB of FTY720-treated SPX LT-$\alpha^{-/-}$mice ($1.33 \pm 0.80 \times 10^7$) was almost identical to the increased number of those cells in the BM ($1.45 \pm 1.47 \times 10^7$), according to the calculating formula estimating that (i) the total number of BM cells could be calculated as 7.9 times the number of cells in two femurs [25] and (ii) the total volume of PB is 2.4 mL [26].

FTY720 treatment suppresses the development of colitis in spleen and LN-null recipients

We previously reported that FTY720 treatment suppresses the development of colitis induced by adoptive transfer of $CD4^+CD45RB^{high}$ T cells [22]. This was legitimate because most $CD4^+CD45RB^{high}$ T cells were naïve $CD44^{low}CCR7^+CD62L^+$ T cells that are accessible to mesenteric LN but at the same time their egress could be inhibited by FTY720 treatment. However, we also demonstrated that FTY720 treatment suppresses the development of colitis in SCID mice that were adoptively transferred with colitogenic LP $CD4^+CD44^{high}CD62L^-IL\text{-}7R\alpha^{high}$ T_{EM} cells obtained from colitic $CD4^+CD45RB^{high}$ T-cell-transferred

SCID mice [22]. This was wholly unexpected because colitogenic LP CD4$^+$ T cells have the characteristics of T_{EM} (CD44^{high}CD62L$^-$) cells that are believed to preferentially migrate to non-lymphoid tissues such as the gut [23, 24], but do not migrate to LN including mesenteric LN. Thus, it remained possible that the migration of colitogenic LP CD4$^+$ T cells is controlled by FTY720

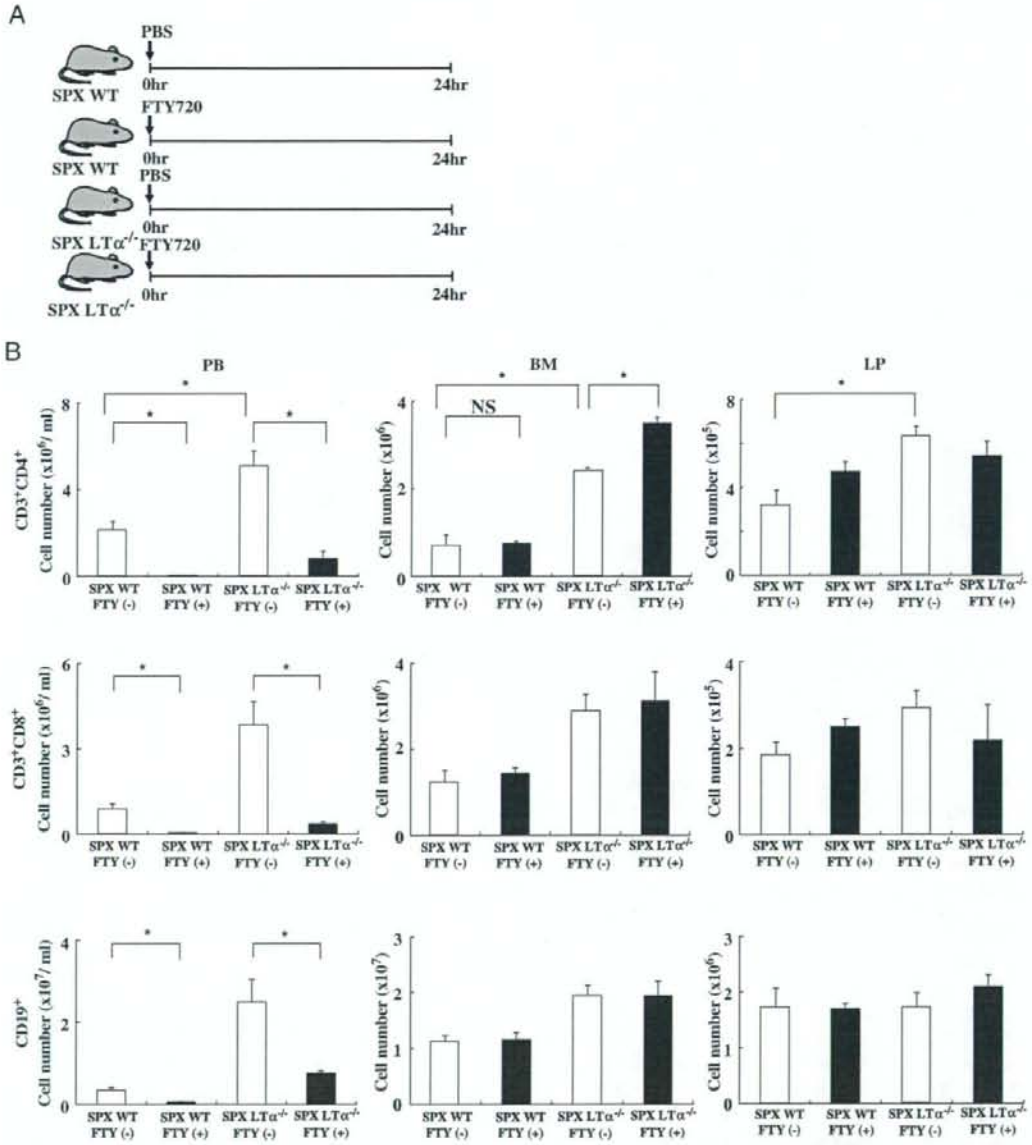

Figure 1. FTY720 treatment induces decrease in PB CD4$^+$ T cells and increase in BM CD4$^+$ T cells in LN/spleen-null mice. (A) FTY720 (1.0 mg/kg) or PBS was i.p. administered to C57BL/6 (WT) or LT-$\alpha^{-/-}$ mice with SPX, and the changes in the absolute numbers of cells were determined at 24 h after treatment. (B) The absolute number of CD3$^+$CD4$^+$ and CD3$^+$CD8$^+$ T cell subsets, and CD19$^+$ B cells in PB, BM, and LP, was determined at 24 h after treatment using flow cytometry. Data are indicated as mean+SEM of six mice in each group. Groups of data were compared by Mann–Whitney U-test. *Indicates statistically significant at $p<0.05$. FTY, FTY720.